RSC Advances

ROYAL SOCIETY OF CHEMISTRY

www.rsc.org/advances

Journal Name

RSCPublishing

COMMUNICATION

Creation of a Superhydrophobic Surface from a Sublimed Smectic Liquid Crystal

Cite this: DOI: 10.1039/x0xx00000x

Dae Seok Kim,[a] Yun Jeong Cha,[a] Hanim Kim,[a] Mun Ho Kim,[b] Yun Ho Kim,[c] Dong Ki Yoon *[a]

Received 00th January 2014,
Accepted 00th January 2014

DOI: 10.1039/x0xx00000x

www.rsc.org/

Dual-scale structures showing superhydrophobic characteristic have been fabricated using sublimable smectic liquid crystals (LCs). Here, toric focal conic domains (TFCDs) of smectic LCs were prepared on micron-sized square pillar patterns. And the layer by layer reconstruction of TFCDs under thermal sublimation process was followed to form nano-scale hemi-cylinders. Based on this dual-scale roughness, the superhydrophobic surface was successfully created with a water contact angle (CA) of ~150° and a low CA hysteresis of ~9°. The resulting superhydrophobic surface is the first application using sublimable LCs, suggesting a new approach for potential applications in LC science and engineering.

Self-cleaning surfaces like lotus leaves show hydrophobic properties such that water droplets running off the surface can carry away contaminants and dirt.[1–2] Such properties have been attractive for potential applications in self-cleaning fabrics,[3] fog-resistant windows,[4] and many other anti-contaminating treatments.[5–6] One of the key self-cleaning applications is the superhydrophobic surface, in which the most important characteristic is dual roughness surface that has coarse-scale feature sizes of around 10 to 20 μm coexisting with finer structures of 100 nm to 1 μm.[7-8] These dual-scale features of nanoscale structures on micron-sized bases are generally difficult and expensive to manipulate using conventional lithographic methods. Thus, self-assembling processes using block copolymers,[9] colloid,[10] soft matters such as LCs,[11,12] have been attractive because of the spontaneous and reversible formation of periodic dual-scale structures over a large area.[13]

Recently, it was found that the fluorinated smectic LC material in previous report can be thermally sublimed in the smectic LC phase.[14] In the presence of layered TFCDs, while a certain amount of LC materials are removed layer by layer at high temperature in the smectic A (SmA) phase, spatial reconstruction around TFCD line defects happens to minimize surface energy of exposed layers to air interface.[14] The resulting topology presents dual-scale feature of concentric ring like structures surrounding core of TFCD where the distance from centre to centre of domes is about 10-15μm with thickness difference (200-250 nm) between terraces (ESI, Fig. S1a, b§). In this paper, we have firstly confirmed that this dual-roughness surface reveals considerably hydrophobic characteristics (CA ~130°) (ESI, Fig. S1c§) and a superhydrophobic surface was manipulated using a square-type pillar-patterned Si substrate with this dual-roughness surface on it, which gives hierarchical structures, resulting in high CA of ~150° and a low hysteresis angle of ~9° which is defined as a difference between advancing angle and receding angle. In order to achieve this goal, low molecular weight molecules that

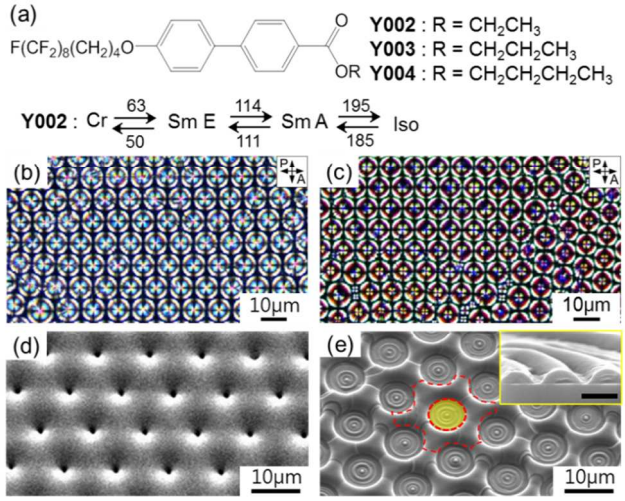

Fig. 1 Molecular structure of LC materials, original TFCDs, and thermally annealed TFCDs on a planar anchoring substrate. (a) Molecular structures and thermal phase transitions of **Y002**. (b) A DRLM image of original TFCDs. (c) A DRLM image of thermally annealed TFCDs. (d) Top-view SEM image of TFCD arrays presenting hexagonal arrays of dimple-like conical shapes. e) SEM image of thermally annealed TFCDs. The red dashed line indicates the outer layers of remaining TFCDs after sublimation and the yellow circle indicates the formation of concentric hemi-cylinders and the inset image shows cross sectional hemi-cylinders (the scale bar is 200nm).

exhibit sublimating property were prepared (ESI, Fig. S2§).[15] Fig. 1a shows the molecular structures of synthetic LCs (**Y002-Y004**) containing a rigid biphenyl group and semi-fluorinated alkyl chains to provide an intrinsic low surface energy for strong water repellence. By measuring the mass loss of LC materials as a function of increasing temperature at a constant heating rate (1 °C min^{-1}), thermogravimetric analysis (TGA) results showed that **Y002**, **Y003**, and **Y004** had thermal sublimating properties (ESI, Fig. S3§). In the case of **Y002**, for example, certain mass loss was found in the SmA LC phase region between 120 °C and 195 °C, although its isotropic temperature is 195 °C. And **Y002** was selected for the manipulation of a superhydrophobic surface because it had the strongest sublimating property among synthetic LC materials.

Y002 shows LC phase transitions of SmA, SmE, and crystal phases during cooling from the isotropic phase (Fig. 1a). As reported in a previous study, hexagonal arrays of TFCDs are generated spontaneously when the sample is prepared on a planar-aligning silicon wafer in the SmA phase. A single TFCD can be considered as a hard sphere whose interactions within the TFCDs are purely steric and repulsive in nature, enabling the formation of hexagonal TFCD arrays (Figs. 1b, d).[16] A depolarized reflective light microscopy (DRLM) image of these TFCDs for **Y002** and other homologs show typical Maltese cross patterns (Fig. 1b and ESI, Fig. S4§), which indicate that the projection of the director field in TFCDs onto the substrate plane was radial within the area bounded by the circular bases of the TFCDs.

As the prepared TFCDs film of **Y002** was thermally annealed at temperature of the SmA phase (140 °C), a certain amount of the film was decreased by sublimation, confirmed through the difference of optical textures and scanning electron microscope (SEM) images before and after sublimation (Figs. 1b-e). In SEM image, the topological feature presents concentric circular hemi-cylinders around the core of TFCD (yellow region in Fig. 1e), which resulted from reorientation of LC molecules in layers of TFCD during sublimation. This resulting structure is attributed to the orientation preference of of the layering directed to minimize the interfacial energy at two antagonistic boundary conditions; layers are normal to the solid interface and parallel to the air interface.[14] This competition is resolved through the formation of hemi-cylinder structures with nano-scale (~150nm) at the LC/air interface as shown in the inset of Fig. 1e. The topological characteristics were quantitatively investigated by atomic force microscope (AFM) for its depth profile; the height and width of hemi-cylinder are ~100 nm and ~200 nm, respectively (ESI, Fig. S5§). As this phenomenon is highly responsive to the annealing temperature, time and other experimental conditions surrounding the system, it has the potential for the manipulation of hierarchical three-dimensional structures under the precise control. Therefore, creating a superhydrophobic film by using this phenomenon is one of the highly achieved applications. So, we have confirmed the relationship between sublimating time at a constant temperature (140 ℃) and hydrophobicity for the LC film through CA measurements of water droplet (All CA measurements were done at room temperature). The value of CA of the TFCD array before thermal annealing was ~106.5°, higher than that of the conventional LC material that has alkyl tails (~78°) and this is resulted from the presence of the semi-fluorinated group in **Y002**.[12]

During thermal annealing at 140℃, the TFCDs were evolved to give concentric hemi-cylinders with TFCDs and CA on its surface was dramatically increased as the annealing time increased, and then reached a maximum after 30 h (ESI, Fig. S1§). Although the CA value of 130° represented a considerably high value of hydrophobic surface, it was not within the superhydrophobic region that mentioned above. We concluded that the simply evolved TFCDs by sublimation on flat substrate did not present a sufficient surface roughness to have air cavities resisting a penetration of water droplet. In order to amplify the surface roughness factor, two kinds of square-type pillared substrates were prepared (l = 5 μm, 10 μm) (Fig. 2a). Both periodic pillar patterned substrates provided the large air cavity to effectively repel water droplet from the surface, in which air pockets remained between the water droplet and the solid surface. **Y002** was loaded on the pillar substrates above isotropic temperature, followed by cooling to SmA phase to generate TFCDs and the dimple centers of TFCDs were mostly attracted to the pillar edges, which can be explained by the "pillar-pinning effect" where the pillar edge confined the straight line defect within core of TFCD to reduce total energy with distorted hexagonal array directed by pillars (ESI, Fig. S4 d, e§).[17] Then, the samples were thermally annealed at 140 °C for 30h to generate the nano-scale structures with TFCDs on these micro-pillars with a certain film thickness. The resulting nano-scale hemi-cylinders were conformal coated over large area in the range of square centimetres, as shown in Figs. 2b, c. The remaining film thickness of the sample after sublimation was below ~1 μm, so that sufficient fractional area for air cavity was retained for high water repellency. Further investigation of the dual-scale roughness on these surfaces was performed with magnified SEM images (Figs.

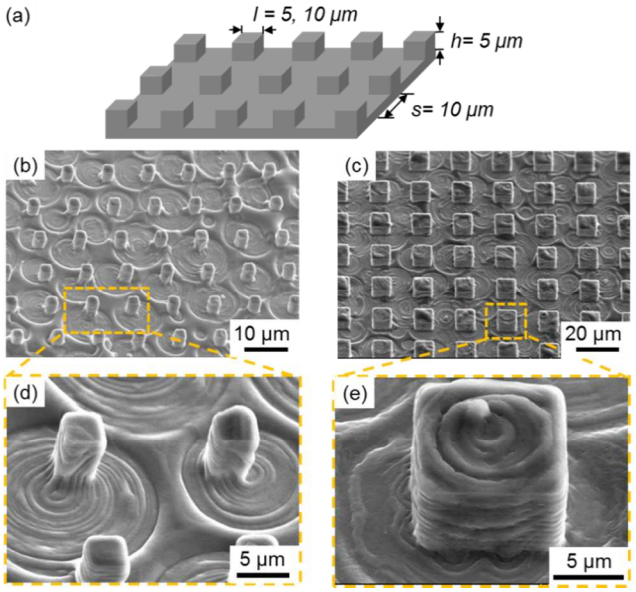

Fig. 2 Nano-scale hemi-cylinders with TFCD arrays on patterned substrates. (a) The bare substrate is described by three parameters; l, s, and h: pattern-width, space, and height, respectively. Two kinds of patterned substrates were used in this process (l = 5 μm and 10 μm). (b, c) The SEM images show that **Y002** was conformally coated with pillar arrays on both substrates through thermal sublimation. (d, e) Magnified SEM images clearly show dual roughness features in which square pillars were enclosed with nano-scale hemi-cylinders.

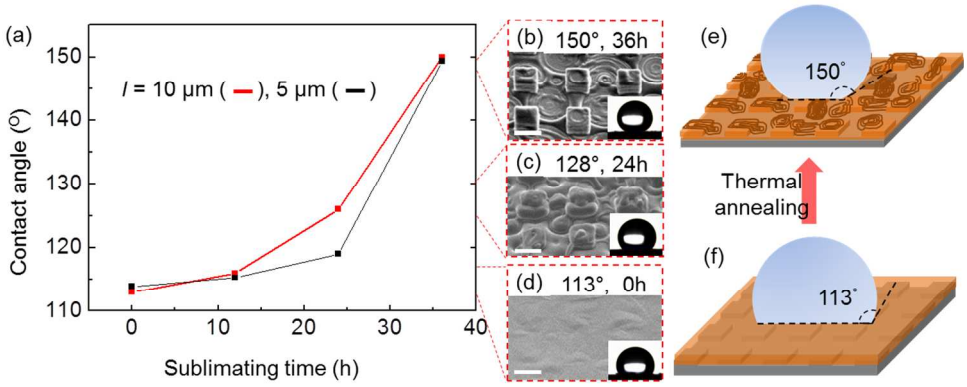

Fig. 3 (a) CA measurements of water droplets on the pillar-patterns with **Y002** as a function of thermal annealing time (b-d) SEM images of hierarchically evolved TFCDs on a square pillared substrate with l = 10 μm. All scale bars are 10 μm. (e-f) Schematic illustrations of the corresponding morphologies of films and water droplets representing the CA value in each state. The insets of (b-d) show water droplets on each surface.

2d, e) and AFM measurement (ESI, Fig. S6§); the nano-scale hemi-cylinders were observed along with micron-scale square pillars, completing the formation of dual-scale surfaces where the scale characteristic of hemi-cylinders are similar to that on flat substrate mentioned above. Fig. 3a shows a graph of the wettability of annealed LC films on two kinds of pillar-patterned surfaces as a function of sublimating time. The TFCDs formed by **Y002** on both 5 μm- and 10 μm-square pillar-patterned Si substrates before thermal annealing had CA of 113.1°, which was consistent with the bulk data (ESI, Fig. S1§). Although the small difference in CA values was caused by pillar patterns, it was reasonable because all the pillar-patterns were buried in the **Y002** and did not have a topographical effect on the CA value (see Figs. 3d, f and insets of ESI, Figs. S4 d, e§). During heating the samples at 140℃, the CA values of both surfaces were dramatically increased as the nano-scale hemi-cylinders on TFCDs were generated, and then CA reached a maximum of ~150° after 36 h. The SEM images of the corresponding evolved surfaces were shown in Figs. 3b-d and the schematic illustrations of initial and final states clearly show the advanced ability for water repellency. The sample on the 5-μm-square pillar-patterned substrate showed the hysteresis was ~13° (CA ~ 149.4°), while the sample on the 10-μm-square pillar-patterned substrate showed a relatively small hysteresis of 9° (CA ~ 150°), indicating that a superhydrophobic surface was successfully created (Figs 3 b, e and ESI, Fig. S7§). Based on these results, we concluded that pillar structures promote the robust micro-scale roughened surface for a reduced water-to-substrate contacting area and our system provides a simple and useful way to create superhydrophobic films.

It is well known that dual-scale surface roughness plays an important role in controlling water repellency.[18] To explain this quantitatively, we turned to the Wenzel model[19] and the Cassie model.[20] The Wenzel model is applicable to a rough substrate, where the advancing CA of water increases with increasing surface roughness and water permeates the surface cavity. On the other hand, the Cassie model is applicable to a system with high receding angle of water at a critical level of surface roughness for which the penetration of water into the surface cavity is unfavourable. So, our approach to manipulate superhydrophobic substrates is presumably applied to the Cassie model because the resulting surfaces show fairly low hysteresis CAs which means that liquid only contacts the solid through the top of the asperities (ESI, Fig. S7§). In the Cassie model, the following formula can be used to show the relationship between surface wettability and surface roughness:

$$\cos\theta_r = -1 + f_s(\cos\theta + 1), \quad (1)$$

where f_s is the fractions of solid–water, thus $1 - f_s$ is air–water contact and θ_r indicates the CAs of a water droplet on rough surface and θ means Young contact angle, fixed by the chemical natures of the material.[21]

In our system, the equation (1) can be rewritten by;

$$\cos\theta_r = f_s \cos\theta_Y - f_a, \quad (1\text{-}1)$$

where f_a (= $1 - f_s$) is air-water contact area and θ_Y is Young contact angle of **Y002**. The θ_Y of fluorinated LC material, **Y002**, is ~113°and the fractional contact areas calculated using the Cassie model {Eq. (1-1)} are given in Table 1. The enhancement of hydrophobicity of these **Y002** films during thermal sublimation can be quantitatively proven to correspond to the values in the table. As previously studied, the dual-scale structure of the lotus leaf surface dramatically increases the surface roughness factor, enabling it to reach the Cassie regime. In the same manner, the surface roughness factor, f_a, of nano-scale hemi-cylinders with TFCDs on 10-μm-square-pillared substrates was consistent with the formation of a superhydrophobic film with water CA of ~150° and CA hysteresis of ~9°. Thus, a dual-scale surface topology arose from nano-scale hemi-cylinders with TFCDs on micro-scale pillars, allow air pockets to exist between the water and the solid surface and making the substrate superhydrophobic.

Sublime time (hr)	l =10μm			l = 5μm		
	CA (deg)	f_s	f_a	CA (deg)	f_s	f_a
0	113.1	0.9260	0.0740	113.9	0.9041	0.0959
12	115.9	0.8536	0.1464	115.3	0.8703	0.1297
24	126.2	0.6265	0.3735	119.0	0.7830	0.1700
36	150.0	0.2036	0.7964	149.4	0.2116	0.7884

Table. 1 CAs and fractional interfacial areas of solid and air contact with a water droplet (f_S and f_a) on square pillar patterned substrates at various sublime time.

Conclusions

In summary, we have manipulated dual-scale roughness structures using sublimable LCs on pillar-patterned substrates to create a superhydrophobic surface. During thermal annealing at the SmLC phase, the low molecular weight LC molecules in the SmA phase were sublimed layer by layer, but were partially and spontaneously reformulated around the centre of TFCDs. In this way, nano-scale circular hemi-cylinders were formed in TFCD arrays. To induce robust micro-scale features in this system, square pillar patterned silicon substrates were introduced, retaining more air gaps for an effective water-repelling function and resulting in an increase in roughness factor to form dual-scale roughness with high air pocket area and a superhydrophobic substrate. The resulting superhydrophobic system using supramolecular LCs with micro-patterns is the first application of sublimable LCs, opening new paths for other three dimensional functional applications.

Acknowledgements

This was supported by a grant from the National Research Foundation (NRF), funded by the Korean Government (MSIP) (2012R1A1A1002486 and, 2012R1A2A2A06046931)

Notes and references

[a] *Graduate School of Nanoscience and Technology and Center for Nature-inspired Technology in KAIST Institute for the NanoCentury, KAIST, Daejeon, 305-701, Republic of Korea. Fax: +82 42 350 1110; Tel: +82 42 350 1116; E-mail: nandk@kaist.ac.kr.*
[b] *Reliability Assessment Center for Chemical Materials, Korea Research Institute of Chemical Technology, Daejeon 305-600, Republic of Korea.*
[c] *Advanced Functional Materials Research Group, Korea Research Institute of Chemical Technology, Daejeon 305-600, Republic of Korea*
† Electronic Supplementary Information (ESI) available: [details of any supplementary information available should be included here]. See DOI: 10.1039/c000000x/

† *Materials and procedures*: **Y002**, **Y003** and **Y004** were synthesized as reported previously (see ESI, Fig. S2§).[12] A pillar patterned Si wafers produced by photolithography were cleaned using acetone and methanol to remove organic/inorganic impurities, followed by rinsing several times with deionized water. And then, a crystalline powder of **Y002** was coated on a square pillar patterned Si wafer by heating to the isotropic temperature (200°C) on a hot stage (LINKAM LTS350) regulated by a temperature controller (LINKAM TMS94). The sample was then cooled to 140°C at a rate of 10°C min-1 and the temperature was maintained at 140°C for ~36 h in order to observe the topographical change of the surface as a function of time.
Fabrication of pillar patterned substrates : Micro-pillars were fabricated on (100) Si wafers using photolithography and reactive ion etching techniques.[22] To control the surface affinity with LC molecules, the channels were chemically cleaned by a mixture of dimethylformide (DMF) and methanol to remove organic/inorganic impurities, followed by rinsing several times with deionized water, which gives highly tangential anchoring of **Y002** on the substrate.
Characterization (H^1-NMR, DRLM, SEM, AFM, and CA goniometry): H^1-NMR (300 MHz) spectra were recorded using a Bruker DRX-300 FT-NMR spectrometer. DSC experiments were carried out with a DSC Q1000 with heating and cooling rates of 5 °C min^{-1}. The samples were observed using a DRLM (LV100POL, Nikon) and a field emission SEM (FE-SEM; Hitachi, S-4800). Surface topological measurements were performed under ambient conditions using AFM (Bruker, Multimode-N3) equipped with a 100 μm scanner in tapping mode. CAs and hysteresis of water droplets on the resulting surfaces were measured using a CA goniometer (Phoenix 300 Touch) and the volume of a water droplet for static measurements was fixed at 5 μL.

1 W. Barthlott and C. Neinhuis, *Planta*, 1997, **202**, 1.
2 D. Quere, Rep. *Prog. Phys*., 2005, **68**, 2495.
3 K. C. Park, H. J. Choi, C. H. Chang, R. E. Cohen, G. H. Mckinley, G. Barbastathis, *ACS Nano*. 2012. **6**. 3789.
4 A. Singh, Y. Lee and W. J. Dressick, *Adv. Mater*., 2004, **16**, 2112.
5 M. Zielecka and E. Bujnowska, *Prog. Org. Coat*., 2006, **55**, 160.
6 S. Srinivasan, V. K. Praveen, R. Philip and A. Ajayaghosh, *Angew. Chem. Int. Ed*., 2008, **47**, 5750.
7 L. Feng, S. Li, Y. Li, H. Li, L. Zhang, J. Zhai, Y. Song, B. Liu, L. Jiang and D. Zhu. *Adv. Mater*., 2002, **14**, 1857.
8 T. Nakanishi, T. Michinobu, K. Yoshida, N. Shirahata, K. Ariga, H. Mo¨hwald and D. G. Kurth. *Adv. Mater.*, 2008, **20**, 443.
9 J. J. Cheng, A. M. Mayes and C. A. Ross, *Nat. Mater.*, 2004, **3**, 823.
10 G. Zhang, D. Wang, Z. Z. Gu and H. Möhwald, *Langmuir*, 2005, **21**, 9143.
11 H. Kim, Y. Yi, D. Chen, E. Korblova, D. M. Walba, N. A. Clark and D. K. Yoon, *Soft Matter*, 2013, **9**, 2793.
12 Y. H. Kim, D. K. Yoon, H. S. Jeong, J. H. Kim, E. K. Yoon and H. T. Jung, *Adv. Funct. Mater*., 2009, **19**, 3008.
13 D. K. Yoon, M. C. Choi, Y. H. Kim, M. W. Kim, O. D. Lavrentovich and H. T. Jung, *Nat. Mater*., 2007, **6**, 866.
14 D. K. Yoon, Y. H. Kim, D. S. Kim, S. D. Oh, I. I. Smalyukh, N. A. Clark and H. T. Jung, *Proc. Natl. Acad. Sci.*, 2013, **110**, 19263.
15 G. Johansson, V. Percec, G. Ungar and J. P. Zhou, *Macromolecules*, 1996, **29**, 646.
16 M. Kleman, *J. Phys*., 1977, **38**, 1511.
17 A. Honglawan, D. A. Beller, M. Cavallaro, R. D. Kamien, K. J. Stebe and S. Yang, *Adv. Mater*., 2011, **23**, 5519.
18 M. Nosonovsky and B. Bhushan, *Adv. Funct. Mater*., 2008, **18**, 843.
19 R. N. Wenzel, *Ind. Eng. Chem*., 1936, **28**, 988.
20 A. Cassie and S. Baxter, *Trans. Faraday Soc.*, 1944, **40**, 546.
21 M. Callies and D. Quere, *Soft Matter*, 2005, **1**, 55.
22 Madou, M. J. Fundamentals of Microfabrication (CRC Press, LLC, 2002)

